Extravascular spaces are the primary reservoir of antigenic diversity in *Trypanosoma brucei* infection

Authors: Alexander K. Beaver[1], Nathan P. Crilly[1], Gracyn Y. Buenconsejo[2], Jill M.C. Hakim[2], Bailin Zhang[2], Bryce Bobb[2], Filipa Rijo-Ferreira[3,4,5], Luisa M. Figueiredo[3], and Monica R. Mugnier[2†].

Affiliations:

[1]Department of Pathology, Johns Hopkins School of Medicine; Baltimore, Maryland, United States of America

[2]Department of Molecular Microbiology and Immunology, Johns Hopkins Bloomberg School of Public Health; Baltimore, Maryland, United States of America

[3]Instituto de Medicina Molecular, Faculdade de Medicina, Universidade de Lisboa, Lisboa, Portugal

[4]Department of Neuroscience, Peter O'Donnell Jr. Brain Institute, University of Texas Southwestern Medical Center; Dallas, Texas, United States.

[5]Division of Infectious Diseases and Vaccinology, Berkeley Public Health Molecular and Cell Biology Department; Berkeley, California, United States of America

[†] Corresponding author. Email: mmugnie1@jhu.edu

Abstract: The protozoan parasite *Trypanosoma brucei* evades clearance by the host immune system through antigenic variation of its dense variant surface glycoprotein (VSG) coat, periodically "switching" expression of the VSG using a large genomic repertoire of VSG-encoding genes[1–6]. Studies of antigenic variation in vivo have focused near exclusively on parasites in the bloodstream[5,7,8], but recent work has shown that many, if not most, parasites reside in the interstitial spaces of tissues[9–13]. We sought to explore the dynamics of antigenic variation in extravascular parasite populations using VSG-seq[7], a high-throughput sequencing approach for profiling VSGs expressed in populations of *T. brucei*. Here we show that tissues, not the blood, are the primary reservoir of antigenic diversity during *T. brucei* infection, with more than 85% of VSGs found exclusively within extravascular spaces. We found that this increased diversity is correlated to slower parasite clearance in tissue spaces. Together, these data support a model in which the slower immune response in extravascular spaces provides more time to generate the antigenic diversity needed to maintain a chronic infection. Our findings reveal the important role that extravascular spaces can play in pathogen diversification.

Main: Every pathogen must contend with the adaptive immune response of its host. *Trypanosoma brucei,* a protozoan parasite and causative agent of human and animal African Trypanosomiasis, has evolved a sophisticated strategy to evade this highly flexible and specific host response[14]. Transmitted by the bite of the tsetse fly, *T. brucei* lives extracellularly in the blood, lymph, and interstitial tissue spaces of its mammalian host[15]. To escape clearance by a continuous onslaught of host antibodies, the parasite periodically "switches" expression of its immunogenic variant surface glycoprotein (VSG) coat to new, antigenically distinct variants[1]. With a genomic repertoire of thousands of different VSG-encoding genes[2–4,6] and the ability to

generate novel VSGs through recombination[5,16], the parasite has an enormous capacity for altering its antigenic profile.

Studies examining *T. brucei* antigenic variation in vivo have focused nearly exclusively on parasites in the blood, revealing complex VSG expression dynamics[5,7,8]. However, it has recently become clear that many, if not most, *T. brucei* parasites inhabit extravascular spaces during both experimental and natural infections[9–13]. Though research has shown that tissue-resident parasites adapt to these environments[11], cause tissue-specific symptoms[15], and are associated with increased disease severity[13], it remains unclear why parasites invade tissue spaces and what role these populations might play in infection.

Two older studies using low-throughput approaches point towards a role for tissue-resident parasites in antigenic variation. These studies found that extravascular parasite populations were antigenically distinct from those in the blood[17,18], suggesting that extravascular spaces could be a site for antigenic variation or, alternatively, that certain VSGs influence the infiltration of or adaptation to tissue spaces, leading to distinct VSG expression in extravascular spaces. Surface proteins involved in antigenic variation influence tissue tropism in other pathogens. In the malaria parasite *Plasmodium falciparum,* for example, the expression of a single *var* gene, *var2csa*, allows for parasites to be sequestered in the placenta[19,20], while antigenic variants of PilE in *Neisseria gonorrhoeae* influence adhesion to different host tissues[21–24]. It is thus plausible that VSG could serve a similar function. Here, we use VSG-seq[7], a targeted RNA-sequencing approach for profiling the VSGs expressed in *T. brucei* populations, to characterize the VSGs expressed by extravascular *T. brucei* parasites. Our results show that extravascular spaces are major reservoirs of antigenic diversity during *T. brucei* infection and that this parasite niche is central to the parasite's ability to continuously outmaneuver the immune system.

Extravascular spaces contain most of the VSG diversity

To investigate how tissue-resident parasites contribute to antigenic variation in vivo, we intravenously infected 12 mice, each with ~5 pleomorphic *T. brucei* EATRO1125 90-13 parasites[25]. We collected blood, then perfused mice with PBS-glucose (Supplementary Fig. 2) and harvested the heart, lungs, gonadal fat, subcutaneous fat, brain, and skin at 6, 10, and 14 days post-infection. For each sample, we extracted RNA and quantified VSG expression using VSG-seq[7]. A single "initiating" VSG (either AnTat1.1 or EATRO1125 VSG-421) dominated expression in both the blood and tissues on day 6 (Fig. 1a). This suggests that *T. brucei* invades tissues before significant VSG switching occurs, which is in line with previous observations[26,27]. At later time points, VSG expression dynamics became more complex, with more VSGs expressed, a unique composition of VSGs in each tissue, and no single dominating variant (Fig. 1a). While we found no evidence for tissue-specific VSGs or VSG sequence motifs (Supplementary Fig. 4), the diversity in tissue spaces was, on average, two to four times higher than the blood (Fig. 1c). This did not correlate with parasite load (Supplementary Fig. 1,3) and was not driven by any specific tissue (Fig. 1d). The overall contribution of tissue-resident parasites to antigenic diversity in a single infection was large: at any time, ~87% of expressed VSGs in any individual infection were found exclusively within extravascular spaces (Fig. 1b). Thus, tissues, not the blood, are the primary reservoirs of antigenic diversity during *T. brucei* infection.

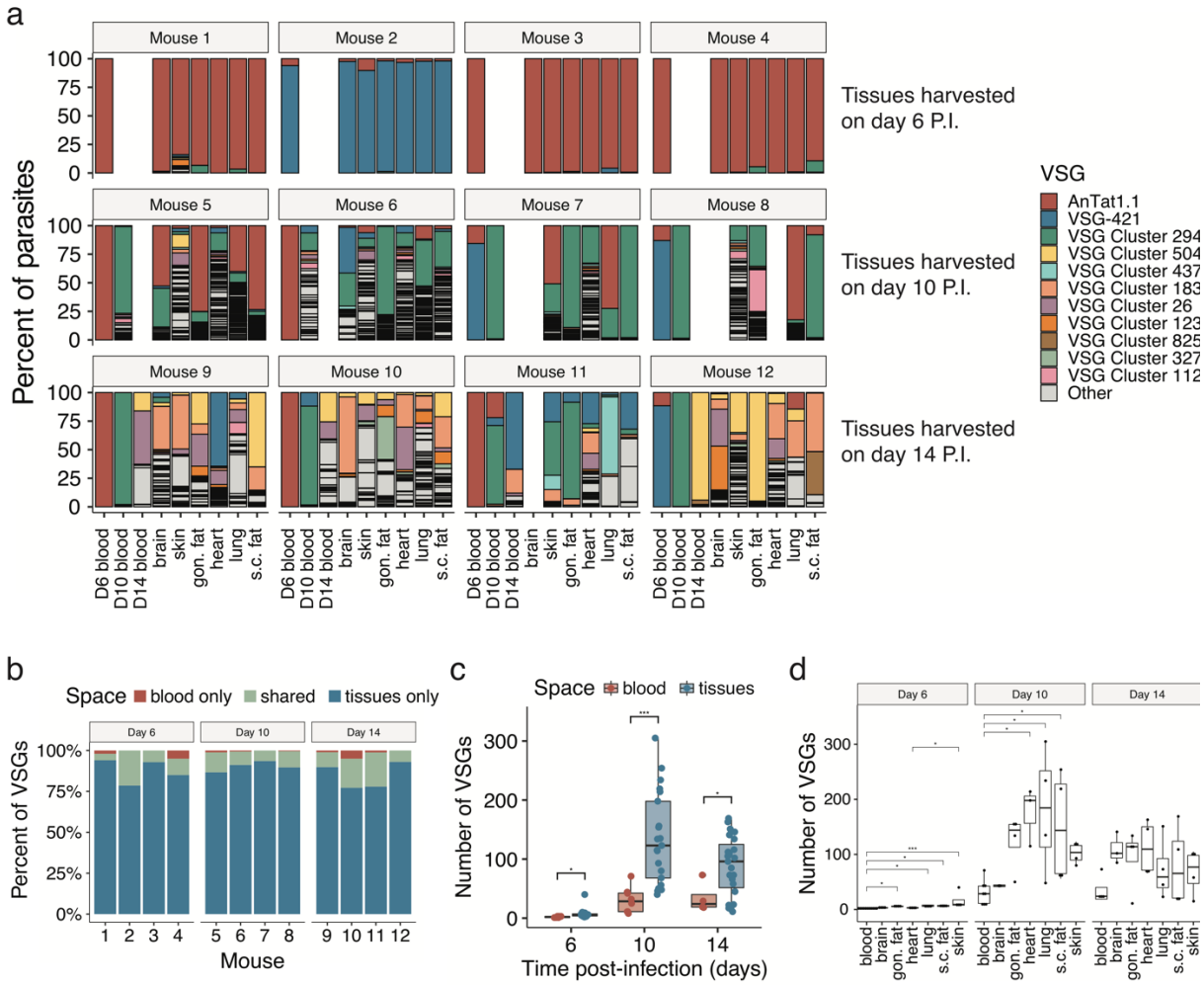

Fig. 1. Extravascular parasites harbor most of the antigenic diversity in an infection. (**a**) The percentage of parasites expressing each VSG within a space. The 11 VSGs with the highest overall expression are colored, and all other VSGs are in grey as "other". Gon. fat = gonadal fat, s.c. fat = subcutaneous fat. (**b**) Stacked bar graphs from each infected mouse representing the percentage of VSGs that were found exclusively within the blood (red), exclusively within tissue spaces (blue), or shared by both the blood and at least one tissue (green). (**c**) Quantification of the number of VSGs found within the blood (red) or tissue spaces (blue) at each time point (Shapiro-Wilk normality test followed by a two-tailed Student's t-test BH corrected). (**d**) The number of VSGs in each tissue space (Shapiro-Wilk normality test followed by a two-tailed Dunnett's test) (For statistical tests *P<0.05, ***P<0.001).

Frequently expressed VSGs first appear in tissue populations

The high antigenic diversity observed in tissues could serve to maintain a chronic infection. If antigenic variation occurs relatively rarely in the bloodstream, then parasites from extravascular spaces might serve as a source of new, antigenically distinct, VSGs. In line with this, tissue spaces contain more "unique VSGs", those VSGs that are expressed exclusively within that

space in an infection, than the blood (Fig. 2a,b). To examine the potential for tissue-resident VSGs to contribute to antigenic variation systemically, we identified VSGs only expressed in tissues on day 6 post-infection and analyzed whether they later appeared within the blood. The majority (74%) of these VSGs were expressed within the blood on day 10 or 14. Analysis of individual VSGs revealed that rare VSGs expressed at low levels exclusively in tissue spaces also have the potential to become ubiquitously expressed within a host (Fig. 2c). In addition to a model in which tissue spaces provide new VSGs to re-seed the blood, it is possible that tissue-resident parasites undergo antigenic variation before blood-resident populations. Therefore, these data could be explained by either a trigger within the tissue environment that induces parasite switching or a differential selective pressure imposed by the tissue environment.

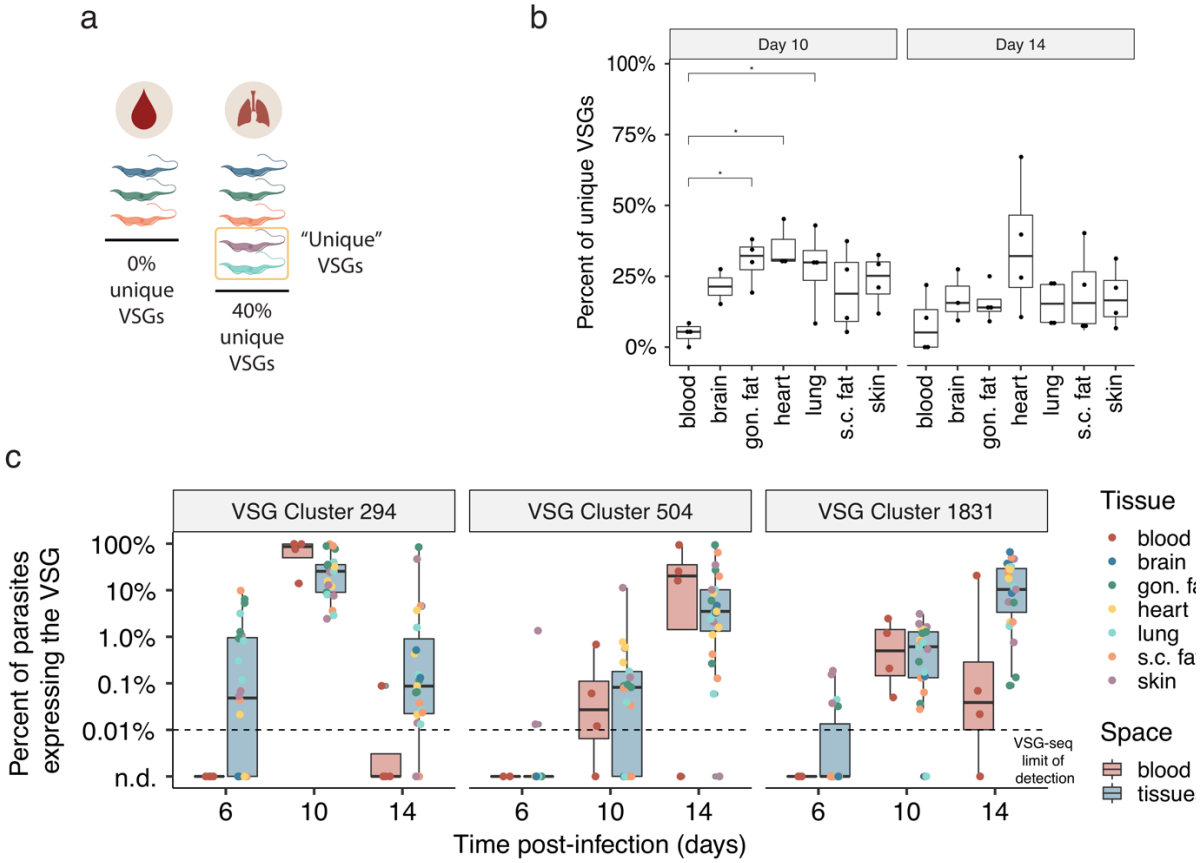

Fig. 2. Tissue-resident parasites express a unique repertoire of VSGs during infection. (**a**) We define "unique" VSGs as those VSGs solely found within a specific space in a mouse (Created with BioRender.com). (**b**) The percentage of VSGs that were unique to one space within a mouse (Shapiro-Wilk normality test followed by a two-tailed Dunnett's test, *P<0.05). Day 6 samples were excluded from this analysis because few VSGs are expressed at this point. Gon. fat = gonadal fat, s.c. fat = subcutaneous fat. (**c**) The expression of three representative VSGs (cluster 294, 504, and 1831) within all samples on days 6, 10, and 14. "n.d" indicates that the VSG was not detected.

VSG-specific parasite clearance is delayed in tissues compared to the blood

101 Indeed, our data suggest that the environment within tissue spaces is distinct from the blood,
102 with parasite clearance occurring at different rates in each space. While parasites expressing the
103 initiating VSG were cleared from the blood by day 10 post-infection, they were not cleared from
104 tissues until at least day 14 (Fig. 3a). This suggests that that the clearance of parasites within
105 extravascular spaces is delayed, but not abolished, compared to the blood. We confirmed this
106 observation by flow cytometry using the tdTomato-expressing "triple reporter" *T. brucei*
107 EATRO1125 AnTat 1.1E cell line[28] (Fig. 3b and 3c). Similar to the increase in antigenic
108 diversity we observed in every tissue space, this delay in clearance was not tissue-specific. Thus,
109 the immune mechanisms influencing extravascular parasite clearance appear to be general
110 features of extravascular spaces.

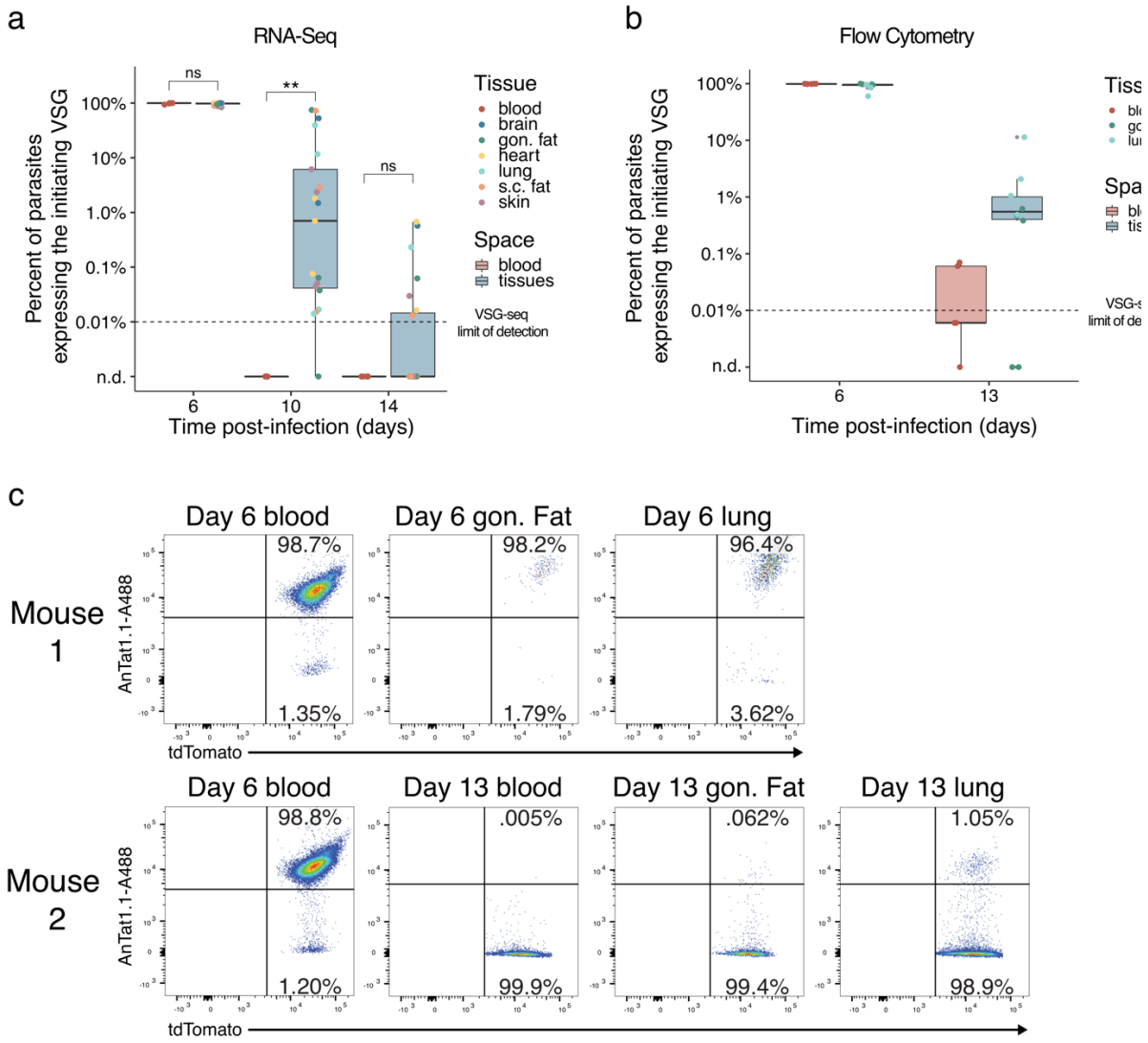

Fig. 3. VSG-specific parasite clearance is slower in tissues than in the blood. (**a**) The percentage of parasites expressing the initiating VSG (AnTat1.1 or VSG-421) at days 6, 10, and 14 post-infection. Tissue samples were grouped together (blue) and compared to blood samples (red) (two-tailed Wilcoxon test, ns = not significant, **P<0.01). "n.d" = not detected, gon. fat = gonadal fat, s.c. fat = subcutaneous fat. (**b**) Quantification of the number of parasites that were tdTomato positive and stained positive for AnTat1.1 by flow cytometry (n = 5 per group). The horizontal dotted line represents the limit of detection for VSG-seq. "n.d" indicates that the VSG was not detected. (**c**) Representative flow cytometry plots from tissues collected from mice infected with chimeric triple marker parasites that express tdTomato constitutively in their cytoplasm. Parasites were stained with anti-AnTat1.1 antibody.

111

112 **Delayed clearance of parasites leads to increased VSG diversity**

113 The increased antigenic diversity in extravascular spaces could be explained by the distinct
114 clearance dynamics we observe, as prolonged survival in tissues could provide more time for

parasites to switch. To test whether there was a link between parasite survival and increased diversity, we sought to interrupt parasite clearance in tissues. Because parasite clearance in the blood (days 8-10) coincides with the appearance of anti-VSG IgM, and parasite clearance in the tissues (days 10-14) coincides with the anti-VSG IgG response[1], we hypothesized that clearance in tissues is dependent on the anti-VSG IgG response. Thus, the loss of IgG might abrogate the clearance of tissue-resident parasites. To test this hypothesis, we infected activation-induced cytidine deaminase (AID) knockout (AID Cre) mice[29], which only produce IgM antibodies (Supplementary Fig. 5), and analyzed blood and tissues from days 6 and 14 post-infection by VSG-seq. As expected, clearance of the initiating VSG was severely delayed in tissues on day 14 in AID$^{-/-}$ mice, suggesting that IgG is important, if not critical, for the clearance of extravascular parasites. This could be explained by the fact that IgM, a bulky pentamer, does not diffuse efficiently into tissue spaces[30,31], while IgG, a monomer, readily diffuses. We also observed a defect in the clearance of blood-resident parasites in AID$^{-/-}$ mice (Fig. 4a). In both blood and tissues where clearance was delayed, more VSGs were detected on day 14 post-infection compared to wild-type (Fig. 4b), revealing a direct relationship between the timing of parasite clearance and VSG diversity. Regardless of their local environment (intra- or extravascular), longer-lived parasite populations generated more diverse sets of VSGs.

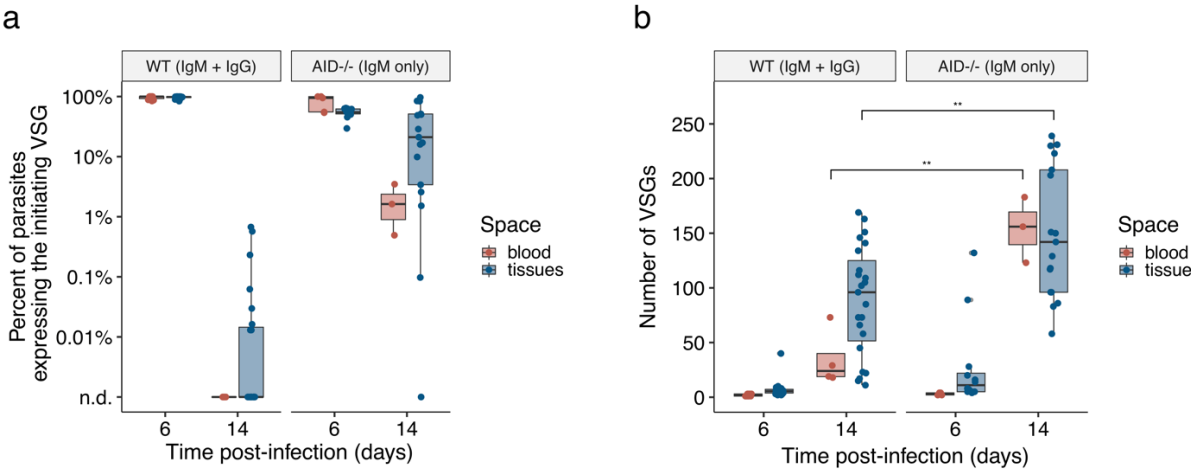

Fig. 4. Delayed parasite clearance correlates with an increase in VSG diversity. (**a**) The percentage of parasites expressing the initiating VSG (AnTat1.1 or VSG-421) in both WT and AID$^{-/-}$ mice. "n.d" indicates that the VSG was not detected. (**b**) The number of VSGs expressed within the blood (red) and tissues (blue) of WT and AID$^{-/-}$ mice (Shapiro-Wilk normality test followed by a two-tailed Student's t-test, **P<0.01).

Discussion

Previous in vivo studies of antigenic variation in *T. brucei* have focused mainly on blood-resident populations. Here we show that extravascular spaces are the primary reservoir of VSGs, accounting for the vast majority of antigenic diversity in any individual infection. The number of VSGs we detected in the blood corroborates previous estimates[5,7,8], while the diversity in tissues is two to four times higher. Our data suggest that this is likely the result of slower clearance

dynamics in extravascular spaces and highlight the role that tissue spaces can play in the generation of genetic diversity during infection.

Although extravascular parasite populations were highly diverse, we saw no evidence of tissue-specific VSG expression. Because parasites invade tissues efficiently before significant VSG switching has occurred, it appears unlikely that any specific VSG is required for tissue invasion. Whether VSGs could influence parasite fitness in specific host spaces is less clear. We measured VSG expression up to day 14 post-infection, at which point tissue-resident populations are just beginning to diverge from one another and the blood. It is therefore possible that, as these populations further evolve, there may be selection for VSGs better adapted to certain tissue spaces.

The striking diversity observed in tissue-resident *T. brucei* populations could be important for the maintenance of natural infections, particularly in wild animals, where pre-existing anti-VSG immunity is more likely to exist. A high switch rate may be required to ensure some parasites successfully evade the host's existing anti-VSG antibody repertoire. In addition, infections in the wild can last for months to years[14,32]. During these long infections, the large reservoirs of VSG diversity found in tissues may be essential for both the establishment and maintenance of a chronic *T. brucei* infection.

Indeed, our data support the idea that the large reservoirs of antigenic diversity in extravascular spaces contribute to systemic infection when parasites re-enter the blood after switching: rare VSGs expressed exclusively in tissues at early time points are expressed in the blood and other spaces later. There is another intriguing explanation for this observation, however. Switching in *T. brucei* is known to be semi-predictable[7,33], and it is possible that tissue-resident parasites simply switch earlier, or more frequently, than those in the blood. In this case, the same VSGs would arise independently in every population without any movement between spaces. While the high vascular permeability observed after the initial stages of infection[13] indicates that parasites likely move back and forth between the vasculature and extravascular spaces, it is exciting to speculate that some aspect of the extravascular environment supplies a molecular or physical stimulus that promotes VSG switching as well.

While the timing of VSG switching could be the result of an environmental trigger, our data suggest that the higher antigenic diversity in extravascular spaces compared to the blood can be explained by the dynamics of the immune response to *T. brucei* in each space. In tissue spaces, we observed slower VSG-specific clearance of parasites than in the blood, potentially providing these populations more time to undergo antigenic variation. Additionally, newly switched parasites are still vulnerable to immune clearance by antibodies against their previous VSG for ~29 hours, so moderate delays in immune clearance could allow more switched parasites to survive[34]. The direct relationship we observed between the timing of parasite clearance and antigenic diversity in $AID^{-/-}$ mice strongly supports this model, with even small delays in clearance rate showing major effects on parasite VSG diversity. Our results show that the production of IgG plays a key role in clearing parasites from tissues, which we propose could be related to the ready diffusion of this molecule within extravascular spaces facilitating parasite clearance. Of course, the local immune response to *T. brucei* is likely complex, with multiple features likely to play a role in parasite detection and clearance. More research will be required to fully understand the nature of the extravascular immune response that results in differential *T. brucei* clearance in tissues.

183 Altogether, our results outline a model in which *T. brucei* parasites "hide" in extravascular
184 spaces to generate new antigenic variants capable of exiting tissues and aiding in systemic
185 immune evasion. Coupled with other recent studies[9–13,35], this suggests a new framework for the
186 progression and pathogenesis of *T. brucei* infections. Instead of being the primary parasite
187 reservoir, the blood may represent a transient population that is regularly re-seeded by
188 extravascular parasites. The vasculature, then, might act as a highway system for movement
189 between the tissue spaces and for eventual transmission back into the tsetse fly.

190 Interfering with the egress from or establishment within tissue spaces might be a strategy for
191 treating *T. brucei* infections or other infections with pathogens that rely on the distinct features of
192 the extravascular environment to diversify. In line with this, one recent study showed that partial
193 inhibition of *T. brucei* tissue invasion using antibodies against P- and E-selectins results in
194 prolonged survival in mice[13]. It is possible that without the proper establishment of parasite
195 tissue reservoirs, overall antigenic diversity is lowered, limiting the parasite's capacity for
196 immune evasion and leading to a decrease in parasite virulence. Defining the dynamics and
197 variation of parasites both within and between spaces, as well as the unique host environment
198 within each tissue space, will be central to understanding how *T. brucei* consistently avoids
199 immune clearance and harnessing this mechanism for disease control.

200 More broadly, these data demonstrate how the different environmental and immune pressures
201 within a host can influence pathogen diversification. This production of genetic heterogeneity
202 within an infection is important for many pathogen virulence processes, including establishing
203 and maintaining infection, facilitating immune evasion, generating drug resistance, and adapting
204 to different host environments. The extravascular environment plays a unique role in promoting
205 pathogen evolution, and *T. brucei* serves as a valuable model for understanding this aspect of the
206 host-pathogen interface.

207

208 **Methods:**

209 <u>Mouse infections and sample collection</u>

210 Female C57Bl/6J (WT, strain# 000664 Jackson Laboratory) or B6.129P2-
211 *Aicda*$^{tm1(cre)Mnz}$/J (AID$^{-/-}$, strain# 007770 Jackson Laboratory)[29] between 7-10 weeks old were
212 each infected by intravenous tail vein injection with ~5 pleiomorphic EATRO 1125 AnTat1.1E
213 90-13 *T. brucei* parasites[25]. Blood parasitemia was counted by tail bleed every 2 days starting on
214 day 4 post-infection (PI) by hemocytometer. Blood (25uL) was collected by a submandibular
215 bleed on days 6, 10, and 14 PI and placed into TRIzol LS. For WT mice, 4 Mice were
216 anesthetized and perfused at days 6, 10, and 14 PI. Infected AID$^{-/-}$ mice were anesthetized and
217 perfused at days 6 (2 mice) and 13 (3 mice) PI. Mice were perfused with 50mL of PBS-Glucose
218 (0.055M D-glucose) with heparin. After perfusion, tissues were dissected and placed
219 immediately into 1mL of RNA later. The heart, lungs, gonadal fat, subcutaneous fat, brain, and
220 skin (ear) were collected.

221 For flow cytometry and immunofluorescence experiments, 7-10 week old female
222 C57Bl/6J mice were infected by intravenous tail vein injection with ~5 AnTat1.1E chimeric
223 triple reporter *T. brucei* parasites which express tdTomato[28]. Blood was collected by a
224 submandibular bleed at each time point. Mice were anesthetized and perfused on days 6 and 13
225 P.I. as discussed above and the gonadal fat and lungs were harvested. All animal studies were
226 approved by the Johns Hopkins Animal Care and Use Committee (protocol # MO22H163).
227

228 VSG-seq sample and library preparation
229 RNA was isolated from blood samples stored in TRIzol LS (ThermoFisher, 10296010)
230 by phenol/chloroform extraction. Tissue samples were weighed and homogenized in TRIzol, and
231 then RNA was isolated by phenol/chloroform extraction. RNA from each sample was DNase
232 treated using Turbo DNase and cleaned up with Mag-Bind® TotalPure NGS beads (Omega Bio-
233 Tek M1378-00). First-strand cDNA synthesis was performed using SuperScript III Reverse
234 Transcriptase and a primer that binds to the conserved VSG 14-mer in the 3′-UTR (5'-
235 GTGTTAAAATATATC-3'). Products were cleaned up using Mag-Bind® TotalPure NGS beads
236 (Omega Bio-Tek, M1378-01). Next, a VSG-specific PCR with Phusion polymerase
237 (ThermoFisher, F530L) was performed using primers for the spliced leader (5'-
238 ACAGTTTCTGTACTATATTG-3') and SP6-VSG 14-mer sequences (5'-
239 GATTTAGGTGACACTATAGTGTTAAAATATATC-3') for 25 cycles. VSG-PCR products
240 were cleaned up using Mag-Bind® TotalPure NGS beads and quantified using the QuBit HS
241 DNA kit (Life Technologies). Finally, sequencing libraries were prepared with the Nextera XT
242 DNA Sample Prep Kit (Illumina) using the manufacturer's guidelines, and libraries were
243 sequenced with 100bp single-end reads on an Illumina HiSeq 2500.
244
245 Tissue QPCR
246 First-strand synthesis was performed with SuperScript III Reverse Transcriptase (Thermo
247 Fisher Scientific, 18080051) and random hexamers primers on tissue RNA samples. QPCR was
248 performed in triplicate using SYBR Green qPCR Master Mix (Invitrogen, 4309155). ZFP3
249 primers were used to estimate parasite load in tissue samples (FW: 5'-
250 CAGGGGAAACGCAAAACTAA-3'; RV: 5'-TGTCACCCCAACTGCATTCT-3'). CT values
251 were averaged between the triplicates and parasite load per mg of tissue were estimated using a
252 standard curve of values from RNA isolated from known numbers of cultured parasites.
253
254 VSG-seq analysis
255 Analysis of sequencing results was performed following the method we reported
256 previously[7], with two changes: no mismatches were allowed for bowtie alignments and each
257 sample was analyzed (assembly, alignment, and quantification) separately. To compare
258 expressed VSG sets between samples, all assembled VSGs were clustered using CD-HIT-EST[36].
259 VSGs with >98% identity to one another were conservatively treated as one VSG. VSGs were
260 then identified by their Cluster number for further analysis. Samples that had less than 100,000
261 successfully aligning reads to VSGs were excluded from further analysis. Four samples, 3 brain
262 and 1 heart, were discarded because fewer than 100,000 reads aligned to VSG (Supplemental
263 Figure 1A). Downstream analysis of expression data and generation of figures was performed in
264 R.
265
266 Analysis of VSG sequence motifs
267 To identify whether there were tissue-specific VSG sequence motifs, the similarity of N
268 terminal sequences from all assembled VSGs were compared. N terminal sequences were
269 identified using a HMMEr scan against a database curated by Cross et al[2,37]. All N termini were
270 compared in an all vs all blast using default parameters. All VSG pairwise comparisons with an
271 e-value higher than 1E-3 were considered sufficiently similar to one another for further analysis.
272 VSGs that were found in a given tissue were binned into that tissue group, and the distribution of

273 the BLAST bitscores in a given compartment was compared against the total population of
274 similar VSGs.
275
276 Flow Cytometry
277 Once mice were perfused, tissues were dissected and washed with HBSS (Hanks
278 balanced salt solution, ThermoFisher Scientific 14175095). Tissue samples were minced and
279 placed in DMEM (ThermoFisher Scientific, 11995065) containing either 1 mg/mL collagenase
280 type 1 (ThermoFisher Scientific, 17100017) for adipose fat or 2 mg/mL collagenase type 2
281 (ThermoFisher Scientific, 17101015) for lung samples. These were then incubated in a 37°C
282 water bath for 1 hour and briefly vortexed every 10 minutes. Next, samples were passed through
283 a 70µM filter and centrifuged at 2600 x g for 8 mins at 4 C, and the cell pellet was taken for
284 antibody staining.
285 Blood samples were collected by submandibular bleed and red blood cells were depleted
286 by magnetic-activated cell sorting (MACS) with anti-Ter-119 MicroBeads (Miltenyi Biotech,
287 130-049-901) following the manufacturer's protocol. Cells were pelleted and washed with HMI-
288 9 media.
289 All samples, both blood and tissues, were stained with Zombie Aqua™ dye at 1:100 in
290 PBS and washed with PBS following the manufacturer's protocol (BioLegend, 423101).
291 Samples were then stained for 10 minutes at 4°C with a rabbit anti-AnTat1.1 polyclonal antibody
292 diluted 1:15,000 in HMI-9 media and washed once with HMI-9 (antibody courtesy of Jay
293 Bangs). Then, secondary antibody staining was performed for 10 minutes at 4°C with Anti-
294 Rabbit IgG conjugated to Alexa Fluor® 488 fluorescent dye (Cell Signaling Technology,
295 4412S). Finally, samples were washed with cold PBS and resuspended in PBS for flow
296 cytometry analysis. Samples were run on a Beckton Dickenson A3 Symphony flow cytometer
297 and analysis was performed using FlowJo (version 10.6.1).
298
299 Immunofluorescence
300 Mice infected with AnTat1.1E chimeric triple reporter *T. brucei* parasites that express
301 tdTomato were sacrificed and perfused as previously described at days 6 and 13 PI. Lung, heart,
302 and gonadal fat were collected and fixed in 4% paraformaldehyde in PBS for 12 hours at 4 C.
303 Post-fixation, tissues were frozen, embedded in O.C.T. Compound (Tissue-Tek), and cut by
304 cryostat microtome into 10µm sections.
305 The following antibodies were applied to sections: rat anti-mouse CD31 (PECAM-1)
306 (SCBT) with goat anti-rat Fluor 488 (CST). Coverslips were mounted using ProLong Gold (Life
307 technologies). Tissues were imaged with 4x, 10x, and 20x objectives using a Nikon Eclipse 90i
308 fluorescence microscope (Nikon) and X-Cite 120 fluorescent lamp (Excelitas) with an ORCA-
309 ER digital CCD camera (Hammamatsu) and ImageJ v1.53 image analysis software. Image
310 collection and analysis followed published guidelines for rigor and reproducibility[38].
311
312 Serum antibody ELISA quantification
313 Blood (25uL) was collected by submandibular bleed on days 0, 6, 10, and 14 PI from
314 mice infected with ~5 pleiomorphic EATRO 1125 AnTat1.1E 90-13 *T. brucei* parasites. Serum
315 was isolated using serum separator tubes (BD Microtainer SST tubes, 365967). IgM and IgG
316 were quantified by ELISA using ThermoFisher IgM and IgG kits following manufacturer
317 protocols (IgG cat# 88-50400-88, IgM cat# 88-50470-88).
318

Statistics and figures

Normality was tested for all Students t-tests and Dunnet's tests analyses and can be found in the code on the repository at https://github.com/mugnierlab/Beaver2022. Nearly all VSG diversity measurements were found to be normally distributed, except for some samples with low VSG counts or sample numbers. We thus assumed normality for all VSG diversity measurements. All reported P-values have been corrected for multiple comparisons using the Benjamini–Hochberg procedure. For all figures with boxplots, the box represents the first (25%) and third (75%) quartiles with a line at the median. Extending lines represent the maximum and minimum values not including outliers that are further than 1.5 times the interquartile range from either end of the box.

Data availability:

Code and data for generating the analysis and figures in this paper are available at https://github.com/mugnierlab/Beaver2022. Raw sequencing data are available in National Center for Biotechnology Information (NCBI) Sequence Read Archive under accession number PRJNA858046.

Acknowledgments: We would like to thank Jay Bangs for supplying us with the anti-AnTat1.1 antibody and Brice Rotureau for providing us with the chimeric triple reporter cell line. We thank Tricia Nilles and Worod Allak at the Becton Dickinson Immunology and Flow Cytometry core at Johns Hopkins Bloomberg School of Public Health for training, support, and technical assistance using the BD FACS Symphony A3. The facility is supported in part by CFAR: 5P30AI094189-04 (Chaisson). Data analysis was carried out at the Advanced Research Computing at Hopkins (ARCH) core facility (rockfish.jhu.edu), which is supported by the National Science Foundation (NSF) grant number OAC 1920103.

Author contributions:

Conceptualization: AB, MRM, LMF, FRF

Methodology: AB, NC, GYB, JH, BZ, BB

Investigation: AB, NC, GYB, JH

Visualization: AB, NC, JH

Funding acquisition: MRM, LMF

Project administration: MRM

Supervision: MRM

Writing – original draft: AB, MRM

Writing – review & editing: AB, GYB, BZ, MRM, FRF, LF

Competing interests: The authors declare that they have no competing interests.

Materials and correspondence: Correspondence and requests for materials should be addressed to Monica Mugnier (mmugnie1@jhu.edu).

References:

358 1. Magez, S. *et al.* The Role of B-cells and IgM Antibodies in Parasitemia, Anemia, and
359 VSG Switching in Trypanosoma brucei–Infected Mice. *PLoS Pathog.* **4**, e1000122 (2008).

360 2. Cross, G. A. M., Kim, H. S. & Wickstead, B. Capturing the variant surface glycoprotein
361 repertoire (the VSGnome) of Trypanosoma brucei Lister 427. *Mol. Biochem. Parasitol.*
362 **195**, 59–73 (2014).

363 3. Müller, L. S. M. *et al.* Genome organization and DNA accessibility control antigenic
364 variation in trypanosomes. *Nat. 2018 5637729* **563**, 121–125 (2018).

365 4. Cosentino, R., Brink, B. & Siegel, T. A phased genome assembly for allele-specific
366 analysis in Trypanosoma brucei. *bioRxiv* 2021.04.13.439624 (2021).
367 doi:10.1101/2021.04.13.439624

368 5. Hall, J. P. J., Wang, H. & David Barry, J. Mosaic VSGs and the Scale of Trypanosoma
369 brucei Antigenic Variation. *PLoS Pathog.* **9**, (2013).

370 6. Hertz-Fowler, C. *et al.* Telomeric Expression Sites Are Highly Conserved in
371 Trypanosoma brucei. *PLoS One* **3**, e3527 (2008).

372 7. Mugnier, M. R., Cross, G. A. M. & Papavasiliou, F. N. The in vivo dynamics of antigenic
373 variation in Trypanosoma brucei. *Science* **347**, 1470–3 (2015).

374 8. Jayaraman, S. *et al.* Application of long read sequencing to determine expressed antigen
375 diversity in Trypanosoma brucei infections. *PLoS Negl. Trop. Dis.* **13**, e0007262 (2019).

376 9. Capewell, P. *et al.* The skin is a significant but overlooked anatomical reservoir for
377 vector-borne African trypanosomes. *Elife* **5**, (2016).

378 10. Camara, M. *et al.* Extravascular Dermal Trypanosomes in Suspected and Confirmed Cases
379 of gambiense Human African Trypanosomiasis. *Clin. Infect. Dis. An Off. Publ. Infect. Dis.*
380 *Soc. Am.* **73**, 12 (2021).

381 11. Trindade, S. *et al.* Trypanosoma brucei Parasites Occupy and Functionally Adapt to the
382 Adipose Tissue in Mice. *Cell Host Microbe* (2016). doi:10.1016/j.chom.2016.05.002

383 12. Carvalho, T. *et al.* Trypanosoma brucei triggers a marked immune response in male
384 reproductive organs. *PLoS Negl. Trop. Dis.* (2018). doi:10.1371/journal.pntd.0006690

385 13. De Niz, M. *et al.* Organotypic endothelial adhesion molecules are key for Trypanosoma
386 brucei tropism and virulence. *Cell Rep.* **36**, 109741 (2021).

387 14. WHO. Control and surveillance of human African trypanosomiasis: Report of a WHO
388 Expert Committee. *WHO Tech. Rep. Ser.* 1–237 (2013).

389 15. Crilly, N. P. & Mugnier, M. R. Thinking outside the blood: Perspectives on tissue-resident
390 Trypanosoma brucei. *PLOS Pathog.* **17**, e1009866 (2021).

391 16. Kamper, S. M. & Barbet, A. F. Surface epitope variation via mosaic gene formation is
392 potential key to long-term survival of Trypanosoma brucei. *Mol. Biochem. Parasitol.* **53**,
393 33–44 (1992).

394 17. Seed, J. R. & Eefron, H. G. Simultaneous presence of different antigenic populations of
395 Trypanosoma brucei gambiense in Microtus montanus. *Parasitology* **66**, 269–278 (1973).

396 18. SEED, J. R., EDWARDS, R. & SECHELSKI, J. The ecology of antigenic variation. *J.*

397 *Protozool.* **31**, 48–53 (1984).

398 19. Salanti, A. *et al.* Evidence for the Involvement of VAR2CSA in Pregnancy-associated
399 Malaria. *J. Exp. Med.* **200**, 1197–1203 (2004).

400 20. Duffy, P. E. & Fried, M. Plasmodium falciparum adhesion in the placenta. *Curr. Opin.*
401 *Microbiol.* **6**, 371–376 (2003).

402 21. Jonsson, A. -B, Ilver, D., Falk, P., Pepose, J. & Normark, S. Sequence changes in the pilus
403 subunit lead to tropism variation of Neisseria gonorrhoeae to human tissue. *Mol.*
404 *Microbiol.* **13**, 403–416 (1994).

405 22. Nassif, X. *et al.* Antigenic variation of pilin regulates adhesion of Neisseria meningitidis
406 to human epithelial cells. *Mol. Microbiol.* **8**, 719–725 (1993).

407 23. Rudel, T., van Putten, J. P. M., Gibbs, C. P., Haas, R. & Meyer, T. F. Interaction of two
408 variable proteins (PilE and PilC) required for pilus-mediated adherence of Neisseria
409 gonorrhoeae to human epithelial cells. *Mol. Microbiol.* **6**, 3439–3450 (1992).

410 24. Virji, M. & Heckels, J. E. The role of common and type-specific pilus antigenic domains
411 in adhesion and virulence of gonococci for human epithelial cells. *J. Gen. Microbiol.* **130**,
412 1089–1095 (1984).

413 25. Engstler, M. & Boshart, M. Cold shock and regulation of surface protein trafficking
414 convey sensitization to inducers of stage differentiation in Trypanosoma brucei. *Genes*
415 *Dev.* **18**, 2798 (2004).

416 26. Turner, C. M., Hunter, C. A., Barry, J. D. & Vickerman, K. Similarity in variable antigen
417 type composition of Trypanosoma brucei rhodesiense populations in different sites within
418 the mouse host. *Trans. R. Soc. Trop. Med. Hyg.* **80**, 824–830 (1986).

419 27. Turner, C. M. R. & Barry, J. D. High frequency of antigenic variation in Trypanosoma
420 brucei rhodesiense infections. *Parasitology* **99 Pt 1**, 67–75 (1989).

421 28. Calvo-Alvarez, E., Cren-Travaillé, C., Crouzols, A. & Rotureau, B. A new chimeric triple
422 reporter fusion protein as a tool for in vitro and in vivo multimodal imaging to monitor the
423 development of African trypanosomes and Leishmania parasites. *Infect. Genet. Evol.* **63**,
424 391–403 (2018).

425 29. Robbiani, D. F. *et al.* Activation Induced Deaminase is required for the chromosomal
426 breaks in c-myc that lead to c-myc/IgH translocations. *Cell* **135**, 1028 (2008).

427 30. Hector, R. F., Collins, M. S. & Pennington, J. E. Treatment of Experimental Pseudomonas
428 aeruginosa Pneumonia with a Human IgM Monoclonal Antibody. *J. Infect. Dis.* **160**, 483–
429 489 (1989).

430 31. BARTH, W. F., WOCHNER, R. D., WALDMANN, T. A. & FAHEY, J. L. Metabolism
431 of Human Gamma Macroglobulins. *J. Clin. Invest.* **43**, 1036 (1964).

432 32. Mehlitz, D. & Molyneux, D. H. The elimination of Trypanosoma brucei gambiense?
433 Challenges of reservoir hosts and transmission cycles: Expect the unexpected. *Parasite*
434 *Epidemiol. Control* **6**, e00113 (2019).

435 33. Morrison, L. J., Majiwa, P., Read, A. F. & Barry, J. D. Probabilistic order in antigenic
436 variation of Trypanosoma brucei. *Int. J. Parasitol.* **35**, 961–972 (2005).

437 34. Pinger, J., Chowdhury, S. & Papavasiliou, F. N. Variant surface glycoprotein density
438 defines an immune evasion threshold for African trypanosomes undergoing antigenic
439 variation. *Nat. Commun.* (2017). doi:10.1038/s41467-017-00959-w

440 35. Trindade, S. *et al.* Slow growing behavior in African trypanosomes during adipose tissue
441 colonization. *Nat. Commun. 2022 131* **13**, 1–13 (2022).

442 36. Fu, L., Niu, B., Zhu, Z., Wu, S. & Li, W. CD-HIT: accelerated for clustering the next-
443 generation sequencing data. *Bioinformatics* **28**, 3150 (2012).

444 37. So, J. *et al.* Trypanosomal variant surface glycoprotein expression in human African
445 trypanosomiasis patients. *bioRxiv* 2021.09.09.459620 (2021).
446 doi:10.1101/2021.09.09.459620

447 38. Lee, J.-Y. & Kitaoka, M. A beginner's guide to rigor and reproducibility in fluorescence
448 imaging experiments. *https://doi.org/10.1091/mbc.E17-05-0276* **29**, 1519–1525 (2018).

449